



Adsorption and catalysis: The effect of confinement on chemical reactions

Erik E. Santiso^a, Aaron M. George^b, C. Heath Turner^c, Milen K. Kostov^a,
Keith E. Gubbins^{a,*}, Marco Buongiorno-Nardelli^{b,d},
Małgorzata Sliwinska-Bartkowiak^e

^a Department of Chemical and Biomolecular Engineering, North Carolina State University, Raleigh, NC 27694-7905, USA

^b Department of Physics, North Carolina State University, Raleigh, NC 27695-8202, USA

^c Department of Chemical and Biological Engineering, University of Alabama, Tuscaloosa, AL 35487-0286, USA

^d CCS-CCM, Oak Ridge National Laboratory, Oak Ridge, TN 37381-6359, USA

^e Institute of Physics, Adam Mickiewicz University, Umultowska 85, 61-614 Poznan, Poland

Available online 9 April 2005

Abstract

Confinement within porous materials can affect chemical reactions through a host of different effects, including changes in the thermodynamic state of the system due to interactions with the pore walls, selective adsorption, geometrical constraints that affect the reaction mechanism, electronic perturbation due to the substrate, etc. In this work, we present an overview of some of our recent research on some of these effects, on chemical equilibrium, kinetic rates and reaction mechanisms. We also discuss our current and future directions for research in this area.

© 2005 Elsevier B.V. All rights reserved.

PACS: 68.90.+g; 82.30.Lp; 82.30.Qt; 82.33.-z

Keywords: Chemical reactions; Confinement; Porous carbons; Molecular modeling

1. Introduction

Many chemical reactions are carried out in micro- and nanoporous materials. These materials can modify both the reaction rates and equilibrium yields in various ways. A beneficial effect of using materials

with small pore sizes is an increase in the area per unit weight, which increases the contact between the catalytic surface and the reactive mixture. There are, however, other effects that can influence chemical reactions in these materials, such as changes in the thermodynamic properties of the reacting mixture due to adsorption, geometrical constraints in pores comparable to the molecular sizes, selective adsorption of reacting molecules, and changes to the potential energy surface that can change the reaction

* Corresponding author. Tel.: +1 919 513 2262;

fax: +1 919 513 2470.

E-mail address: keg@ncsu.edu (K.E. Gubbins).

mechanism. In most cases, it is difficult to assess the relative importance of each one of these effects. Experimental measurements usually reflect a combination of all of them, and it is usually impractical to perform experiments to study each effect separately. Furthermore, the relative importance of each factor will likely be very different for different kinds of chemical reactions, and the experiments would have to be repeated many times. These difficulties make the problem attractive for molecular simulation studies. A clear understanding of the influence of each factor on a particular chemical reaction can provide useful information for the design of better catalytic materials, which can not only enhance the reaction yields but also provide a partial separation of the reaction products.

During the past few years, we have carried out several studies on the effect of confinement on both equilibrium yields and reaction mechanisms for various chemical reactions in nanoporous materials, and have gained insight into the influence of the effects mentioned above on these reactions. In this work, we present an overview of the results we have obtained, and discuss some possible new directions for research.

The rest of this work is structured as follows: in Section 2, we discuss results on the effect of confinement on equilibrium yields for various chemical reactions; in Section 3, we discuss results on the influence of confinement in nanoporous carbons on both rate constants and reaction mechanisms; finally, in Section 4, we discuss some current research directions and give some suggestions for future research in the area.

2. Effect of confinement on chemical equilibrium

One of the most evident ways in which confinement can affect a reactive system is by altering the thermodynamic properties of the reacting mixture. Interactions between the porous substrate and the components of the mixture can modify the density of the adsorbed phase, and this would have a direct effect on systems where the number of molecules changes upon reaction. For mixtures in which the interactions with the adsorbent are different for each component, selective adsorption can also drive the equilibrium towards the reactants or the products. These effects

can occur regardless of the strength of the catalytic effect of the porous material, as they are dictated not by the kinetics but by the thermodynamics. Therefore, a study of the interplay between adsorption and chemical equilibrium is crucial for the design of a good catalytic material—an enhancement of the reaction rate is not useful if the equilibrium yield is small.

In this section, we discuss some of our results on the effect of confinement on the equilibrium yield of three different chemical reactions: the dimerization of nitric oxide, the synthesis of ammonia from nitrogen and hydrogen, and the esterification reaction between ethanol and acetic acid. The first two reactions provide good examples of the effect that a change in the density of the reactive mixture can have on the equilibrium yield, and the latter shows more specifically the effect of selective adsorption.

2.1. Methods

All the results shown in this section were obtained by using the reactive Monte Carlo (RxMC) method [1,2]. RxMC is a method specifically tailored to obtain equilibrium properties of reactive systems. In a RxMC simulation, a set of “forward” and “backward” reaction moves are added to the “standard” Monte Carlo moves in order to get the system to chemical equilibrium. In these reactive moves, reactant molecules are randomly chosen and replaced with product molecules (or vice versa). The acceptance probability for a reactive move can be derived from statistical mechanics, and is given by the expression:

$$P_{\text{acc}} = \min \left\{ 1, \exp(-\beta\Delta u) \prod_{i=1}^c q_i^{v_i} \frac{N_i!}{(N_i + v_i)!} \right\} \quad (2.1)$$

where Δu is the change in the configurational energy due to the reactive move, $\beta = 1/kT$, c is the number of components, and N_i , q_i and v_i are, respectively, the number of molecules, the molecular partition function and the stoichiometric coefficient in the reaction of component i . The RxMC method has been shown to reproduce correctly the experimental equilibrium yields in the bulk for all the reactions considered in this work [3–5].

The porous carbon models that constitute the adsorbent in the results shown in the following

sections include a carbon slit-pore modeled using the 10-4-3 Steele potential [6], model carbon nanotubes of the armchair type, a realistic carbon model reconstructed from X-ray diffraction data using the reverse Monte Carlo method [7], and an activated carbon slit-pore including carboxyl sites modeled using the method of Shevade et al. [8]. Further details of these models can be found in [3–5,9].

2.2. Dimerization of nitric oxide and ammonia synthesis

The dimerization of nitric oxide (NO) is a good candidate for studying the effect of confinement for several reasons. First, the reaction and the molecules involved are quite simple to model, as long as the main goal is the estimation of thermodynamic properties. There are good intermolecular potentials [1] for both NO and the dimer (NO)₂, and experimental data is available for the dimerization reaction in the bulk phase [10–12], in activated carbons [13], and in carbon nanotubes [14]. It is particularly interesting to study the effect of confinement on this reaction because a quite dramatic increase of the dimer yield in the pores has been reported in experimental measurements [13,14].

The ammonia synthesis reaction, $N_2 + 3H_2 \leftrightarrow 2NH_3$, is also a good model reaction for studying the effect of confinement. Since ammonia is one of the synthesis chemicals most commonly produced industrially, there is plenty of reference data for the bulk reaction [15]. There is, however, no information regarding the equilibrium reaction yield in small pores. Since this is a very commercially important reaction, it is worthwhile to study the possible effect of confinement on its equilibrium yield.

Fig. 1 shows the equilibrium composition of a reacting mixture of NO and (NO)₂ as a function of temperature in slit pores of sizes ranging from 0.80 to 1.59 nm [3]. The bulk gas phase composition is also shown for comparison purposes. The data in Fig. 1 correspond to a constant bulk pressure of 0.16 bar. These results show a large effect of confinement on the equilibrium yield of the reaction, with increases on the dimer composition up to a factor of 40 at the lower temperatures. The main reason for this effect is the increased density of the pore phase, due to the attractive interactions between the NO molecules and the carbon

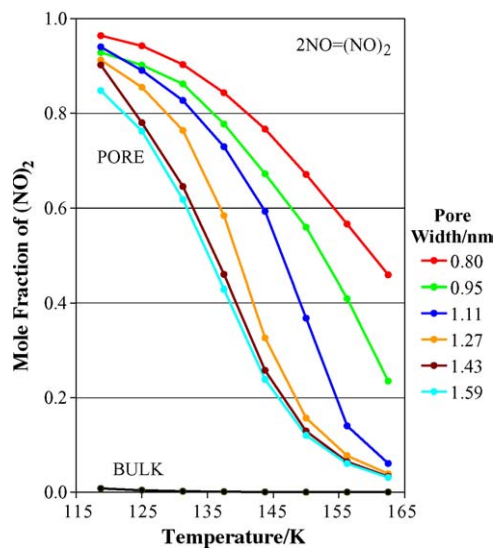


Fig. 1. Effect of confinement on the NO dimerization in carbon slit pores of various sizes [3]. The results correspond to a bulk phase pressure of 0.16 bar.

walls. For the smaller pores, these interactions become more important [3] and the increase in yield of the dimer is larger. Similar results were obtained for NO confined within carbon nanotubes.

The effect of confinement on the equilibrium yield of the ammonia synthesis reaction for carbon slit pores and carbon nanotubes is shown in Fig. 2 as a function of temperature and pore size [3,4]. The data in this figure correspond to a bulk gas phase pressure of 100 bar, and the bulk yield is also shown for comparison. In this case, the enhancement in yield results largely from selective adsorption of the

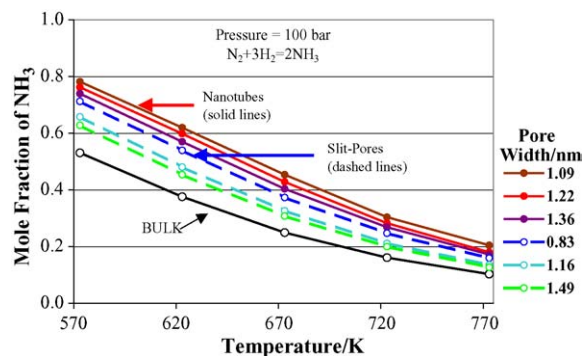


Fig. 2. Effect of confinement on the ammonia synthesis reaction in slit pores and carbon nanotubes of various sizes [4].

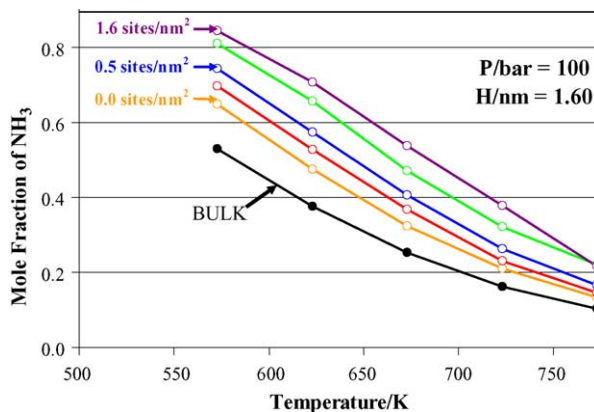


Fig. 3. Effect of active site concentration on the ammonia synthesis reaction [4].

ammonia product. There is also an enhancement of the equilibrium yield due to the particular geometry of the pore structure: the ammonia conversion is larger for nanotubes than for slit pores of comparable size. The increase in yield due to confinement in this case is smaller than in the case of the nitric oxide dimerization, but this is largely due to the much higher temperatures, and to the fact that the bulk phase pressure is much larger and hence there is significant conversion also in the bulk.

In Fig. 3 is shown the equilibrium yield of the ammonia synthesis reaction in activated carbon slit pores for different activated site densities [4]. The active sites are modeled as carboxyl groups. The results in Fig. 3 correspond to a bulk phase pressure of 100 bar and a pore width of 1.60 nm. The figure shows that an increase in the density of active sites further improves the ammonia yield, due to the favorable electrostatic interactions between ammonia and the carboxyl groups.

We also considered the effect of pore heterogeneity on the ammonia synthesis reaction [4], using the realistic carbon model of Pikunic et al. [7]. The results show a very small effect of the pore heterogeneity on the ammonia yield, probably due to the high temperatures considered in the simulations.

2.3. Esterification of acetic acid and ethanol

The reactions considered in the previous section, $N_2 + 3H_2 \leftrightarrow 2NH_3$ and $2NO \leftrightarrow (NO)_2$, have two important common features: (1) the number of moles

decreases upon reaction; and (2) there is an attractive interaction between the reacting molecules and the adsorbent, causing the adsorbed phase to have a significantly higher density than the bulk phase. The combination of these two factors naturally causes an enhancement of the equilibrium yield, as the increased density of the adsorbed phase displaces the equilibrium to the side with a lower number of moles. It would be interesting to consider now a reaction for which this is not the case, i.e. where there is no change in the number of moles upon reaction. In such a case the most important factor is likely to be the difference between the wall–fluid interactions among different species in the reacting mixture.

The esterification reaction of acetic acid and ethanol to produce ethyl acetate, $CH_3COOH + C_2H_5OH \leftrightarrow C_2H_5OOCCH_3 + H_2O$, is a common industrial process in the synthesis of organic solvents. There is experimental evidence [16] that when this reaction is carried out in porous materials, the selectivity towards ethyl acetate depends on the adsorbent used. Therefore, it is likely that the fluid–wall interactions play a role in determining the equilibrium yield for this reaction in pores.

The equilibrium yield of the esterification reaction in both smooth slit pores and activated carbon slit pores, as obtained from RxMC simulations, is shown in Fig. 4 [5]. The results correspond to a temperature of 523.15 K and a bulk phase pressure of 1 bar. The activated site density for the activated carbon results is 1.82 sites/nm². In the figure the bulk equilibrium yield is shown for comparison.

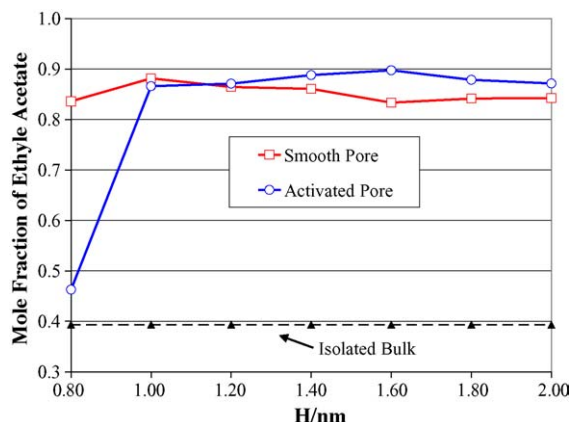


Fig. 4. Effect of confinement on the esterification reaction [5]. The results correspond to a temperature of 523.15 K and a bulk phase pressure of 1 bar. The concentration of active sites in the activated pore is 1.82 sites/nm². H represents the pore width.

The results in Fig. 4 show that there is a significant enhancement of the equilibrium yield for the confined fluid, as the mole fraction of the ester is more than doubled in the pore phase. This difference was shown [5] to be due to the selective adsorption of the ester, which has a more favorable fluid–wall interaction than the other components in the mixture.

In Fig. 4, it can also be seen that the addition of active sites has a relatively small impact on the equilibrium yield, except for the smallest pore, where it significantly inhibits the reaction. In the simulations no correlation was found between the positions of the active sites and the ethyl acetate molecules, suggesting that the main reason for this result is just a geometric effect. The presence of the –COOH groups actually makes the effective pore size smaller, as it reduces the space available for the other molecules. Thus, it is reasonable that the equilibrium yield is slightly larger for the activated carbon in the wider pores: the yield is equivalent to that on a smaller unactivated pore. The decrease in equilibrium yield for the activated carbon in the smaller pore is likely due to the fact that the carboxyl groups do not leave enough space for the ethyl acetate to form, thus having now the opposite effect.

2.4. Concluding remarks

The results in the previous sections illustrate two important effects that can influence chemical reactions

within a porous material. The first two examples illustrate how a change in the density of the pore phase with respect to its bulk value can have a direct impact on the equilibrium yield for reactions where the number of moles changes upon reaction. In the second example we considered a system for which this is not the case, so that density effects are unimportant, and we show that still there can be an important change in the equilibrium yield due to selective adsorption of one of the components in the reacting mixture. All these results indicate that it is possible to enhance (or inhibit) significantly a particular reaction just by a proper choice of the reactive medium.

There are, however, still important questions to address. The results shown so far correspond to thermodynamic equilibrium situations. From a practical point of view it is also important to consider the kinetic aspects: even if the equilibrium yield is greatly enhanced, it may take too long to reach the equilibrium state. Therefore, the next logical step is to consider the effect of confinement on chemical reaction kinetics. This is the subject of the next sections.

3. Effect of confinement on chemical kinetics and mechanism

The influence of confinement on rates is a much more complicated problem, as the equilibrium state is only a function of the properties of reactants and products, whereas the rate depends on how the reactants evolve to become the products. As for chemical equilibrium, there are different ways in which confinement can affect the rate of a reaction. Besides the purely thermodynamic factors, confinement can also influence the reaction rate by changing the size of the activation energy barrier for the reaction, or even completely changing the reaction mechanism. Since there are many possibilities depending on the nature of the reacting mixture and the adsorbent, we have decided to first examine simple cases where we can isolate the influence of one different effect at a time. This allows us to judge the relative impact of each effect in each given type of reaction, and to build a picture that could be useful later for the design of catalytic supports.

In this section, we discuss some results on the effect of confinement on the kinetics of three different chemical reactions: the decomposition of hydrogen iodide, the rotational isomerization of 1,3-butadiene, and the unimolecular decomposition of formaldehyde. The first example shows how the RxMC methodology can be extended to estimate reaction rates in confinement. The second example shows the impact that the reduced dimensionality of a small pore can have on chemical reactions requiring a three-dimensional motion of a molecule. Finally, the third example illustrates the catalytic effect of a carbon wall on a reaction involving charge displacement.

3.1. Methods

The decomposition of hydrogen iodide, $2\text{HI} \leftrightarrow \text{H}_2 + \text{I}_2$, was studied in carbon slit pores and nanotubes [17] using a combination of the RxMC method and the transition state theory (TST) of Eyring [2,18,19]. The reaction rate was estimated by equilibrating a mixture of hydrogen iodide and the transition state species for the reaction, $(\text{HI})_2^\ddagger$, with the same structure as in the bulk reaction. Then the rate constant was calculated from the expression:

$$k_{\text{obs}} = \frac{k_{\text{B}}T}{h} \frac{c^\ddagger}{c_{\text{HI}}^2} \quad (3.1)$$

where k_{B} is Boltzmann's constant, h is Planck's constant, T is the temperature, and c^\ddagger and c_{HI}^2 are the equilibrium concentrations of the transition state and hydrogen iodide. In practice, it was necessary to introduce a bias to increase the probability of accepting the "forward" reaction steps. The rate constant was corrected afterwards to remove the effect of this bias. Further details of the methodology can be found in [9].

The methodology discussed for the decomposition of hydrogen iodide, although efficient, involves the assumption that the transition state structure is the same in the pores and in the bulk. This assumption will likely break down for pores of sizes comparable to the molecular size, or for porous materials which can interact strongly with the reactive mixture and therefore alter the reaction mechanism. In order to study these effects, we carried out ab initio calculations for the rotational isomerization of 1,3-butadiene and the unimolecular decomposition of formaldehyde

in carbon slit pores. These calculations were done using plane-wave density functional theory (DFT) [2,20] with the Becke–Lee–Yang–Parr (BLYP) exchange-correlation functional [2,21,22] and ultrasoft pseudopotentials [23]. The results for the isomerization of 1,3-butadiene were obtained with the CPMD code [24], and the ones for formaldehyde were obtained with the pwsfc code [25]. The carbon pores were represented by graphene walls containing 32 carbon atoms, in a hexagonal unit cell. The structures of transition states in the isomerization of 1,3-butadiene were optimized using the rational function optimization (RFO) method [26,27], and the reaction pathways in the decomposition of formaldehyde were obtained using the nudged elastic band method (NEB) [28–30]. Further details of the simulation methods can be found in [31].

3.2. Decomposition of hydrogen iodide

The reaction rate for the decomposition of bulk hydrogen iodide at 573.15 and 594.55 K, as a function of the initial HI concentration, is shown in Fig. 5. The results obtained using the RxMC-TST methodology outlined in the previous section are compared with experimental results from [32]. Considering the scattering of the experimental data, especially in the region of low concentrations, the agreement between our simulations and the experimental results is quite good, thus validating the use of the RxMC-TST methodology for this reaction.

The effect of confinement on the reaction rate for the dissociation of hydrogen iodide, $2\text{HI} \leftrightarrow \text{H}_2 + \text{I}_2$, is shown in Fig. 6. The simulations were carried out in both slit pores and carbon nanotubes, with a temperature of 573.15 K and pressures up to 200 bar. It is clear from this figure that confinement within small pores causes a large enhancement of the reaction rate, with increases up to a factor of 47. Part of this effect is due to the increased density of the pore phase, which favors the formation of the transition state species, as this leads to a decrease in the total number of moles. Another factor that causes an increase in the reaction rate is a more favorable fluid–wall interaction between the $(\text{HI})_2^\ddagger$ transition state species and the pore walls. Therefore, we see here a combination of the factors we discussed in Sections 2.2 and 2.3.

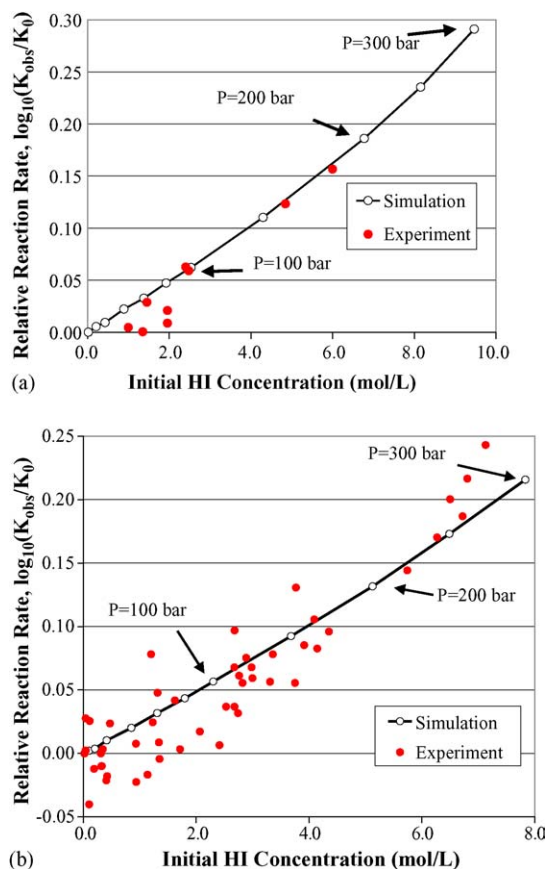


Fig. 5. Reaction rate of the hydrogen iodide decomposition at (a) 573.15 K and (b) 594.55 K [9]. The open circles correspond to our simulation results, and the closed circles to the experimental results in [32]. The pressure corresponding to three of the HI concentrations is shown.

It is clear from the results in this section that a reasonable picture of the effect of confinement on the rate of a chemical reaction can be obtained by considering the interactions of the activated complex with the porous material. This picture, of course, will not give good results for cases where the quasi-equilibrium approximation of TST is not valid (reactions with small barriers, at very low temperatures, etc.). There is, however, another issue to consider: if the fluid–wall interactions are strong enough to have an effect on the intramolecular degrees of freedom, it is possible that the transition state structure is different in the confined system. Furthermore, the reaction mechanism can be completely different. This kind of problem will be considered in the following sections.

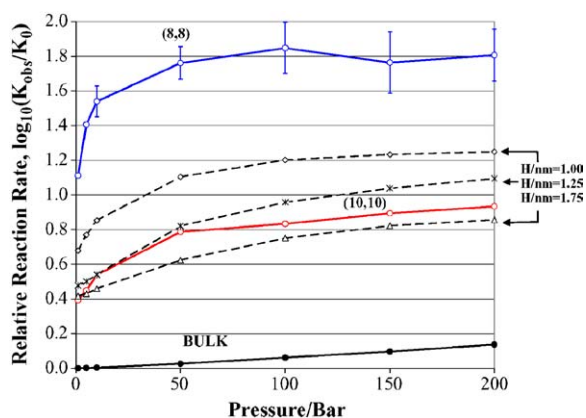


Fig. 6. Effect of confinement in slit pore carbons (dashed lines) and carbon nanotubes (solid lines) on the rate of dissociation of hydrogen iodide [9]. The results correspond to a temperature of 573.15 K.

3.3. Isomerization of 1,3-butadiene

The simplest kind of chemical reaction that can be affected by geometrical constraints is an isomerization. Since isomerizations often involve a three-dimensional rearrangement of the atoms in the molecule, the reduced dimensionality of the porous space is likely to have an effect on the reaction energy profile and, possibly, on the structure of the stable states. The case of 1,3-butadiene is particularly interesting because the structure of the high-energy conformer is determined by an interplay between the steric hindrance between the methylene end groups and the stabilization due to bond conjugation in the planar structures. This makes it likely that the structure of this conformer will be affected by the constrained geometry of the pore. The isomerization of 1,3-butadiene in the bulk has also been extensively studied both experimentally [33–38] and theoretically [39–42], which allows us to validate our results.

Fig. 7 shows the potential energy for 1,3-butadiene as a function of the dihedral angle between the four carbon atoms, both in the bulk and in carbon slit pores of widths ranging from 6.9 to 9 Å [31]. The barrier for the conversion from the *s-trans* (torsion angle = 180°) to the *s-gauche* (torsion angle = 30°) in the bulk is predicted by DFT-BLYP to be 7.5 kcal/mol, and the torsion angle for the transition state is 100.4°. Results from coupled-cluster CCSD(T) calculations [42] show the barrier to be 6.3 kcal/mol and the transition state

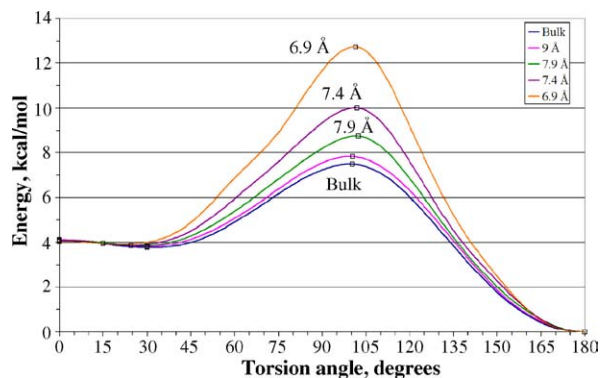


Fig. 7. Potential energy of 1,3-butadiene in the bulk and in carbon slit pores with widths ranging from 6.9 to 9 Å [31]. Stationary points are marked with squares.

torsion angle to be 100.7° . The disagreement between the transition barriers obtained by the two methods can be explained by the poor representation of conjugate bond breaking given by the Becke functional [42,43]. A solution to this problem would be to repeat the calculations with a higher-level method, but this would make the computational cost for the pore calculations far larger. The barrier for the automerization of the *s-gauche* conformer is predicted by DFT-BLYP to be 0.34 kcal/mol in the bulk, in reasonably good agreement with the CCSD(T) value of 0.42 kcal/mol from [42].

For pore sizes greater than ~ 10 Å (roughly three times the size of the molecule), the energy profile is essentially the same as that in the bulk. Nevertheless, as soon as the pore size goes below this value, the barrier for the conversion of *s-trans*-1,3-butadiene to *s-gauche*-1,3-butadiene increases fast, becoming ~ 1.85 times the bulk value at a pore size of 6.9 Å.

Fig. 8 gives a more detailed view of the region of small torsion angles, showing a more interesting feature of the results. For pore sizes below 7.9 Å, DFT-BLYP predicts that the structure of the stable *s-gauche* conformer drifts toward smaller values of the torsion angle. Even though the potential energy valley becomes shallower and wider, thus inducing a large error in the value of the equilibrium torsion angle, it is clear that the structure of the high-energy conformer is being influenced by the steric hindrance imposed by the pore walls. The energy barrier for the automerization of the *s-gauche* conformer is also reduced compared to the bulk value, with DFT-BLYP predicting a barrier of less than 0.1 kcal/mol at the

6.9 Å pore. This is another instance of the effect discussed in the previous section: the transition state for the *s-gauche*–*s-gauche* automerization is the *s-cis* structure (torsion angle = 0°) which, being planar, fits better in the narrow pores. This makes the automerization more likely to happen at small pore widths.

3.4. Unimolecular decomposition of formaldehyde

The results shown in the previous section show how the geometrical constraints imposed by the porous material can affect a chemical reaction. The effect is believed to be entirely due to confinement, since the perfect graphene walls are extremely stable chemically and thus, are unlikely to have a catalytic effect on the reaction. There is, however, evidence that the presence of a graphene wall or a carbon nanotube nearby can have a catalytic effect on reactions involving a displacement of charge [44]. In this section, we consider this possibility for the unimolecular decomposition of formaldehyde, $\text{HCHO} \leftrightarrow \text{H}_2 + \text{CO}$. In this reaction, there is a displacement of charge along the C–O bond, which can be helped by the high polarizability of the graphene walls. The reaction is also a good candidate to later study the effect of selective adsorption, as the relative affinity of the components in the reactive mixture to the walls is significantly different.

The reaction pathway for the decomposition of formaldehyde in the bulk, as obtained from an NEB calculation with five images, is shown in Fig. 9. The energy barrier for the decomposition is found to be 80.3 kcal/mol, in excellent agreement with the

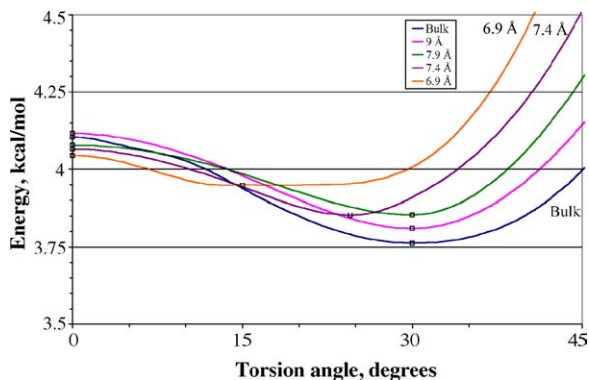


Fig. 8. Potential energy of 1,3-butadiene for small torsion angles. The squares mark the location of the stable *s-gauche* conformer.

experimental value of 79.2 ± 0.8 kcal/mol [45]. This indicates that DFT-BLYP gives a good representation of the energy landscape for this particular reaction.

The energy profile for the dissociation of formaldehyde close to a graphene wall, as obtained from an NEB calculation with 11 images, is shown in Fig. 10. The bulk energies are also indicated in the figure as a reference. The energy barrier is reduced by 1.5 kcal/mol with respect to the bulk value, which indicates that there is a catalytic effect from the graphene sheet, but this effect is very small compared to the size of the barrier. The products are also stabilized by 3.8 kcal/mol with respect to the bulk value, indicating that the effect on the equilibrium distribution of reactants and products would be more important for this reaction.

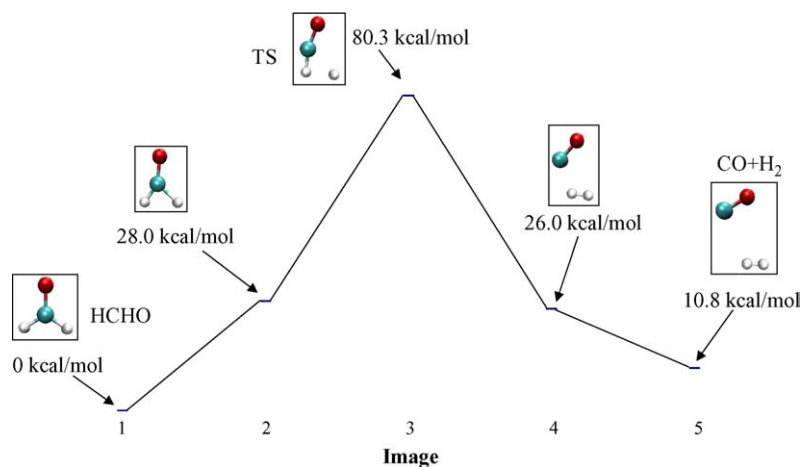


Fig. 9. Energy profile for the unimolecular decomposition of formaldehyde in the bulk. Image 3 is the transition state.

3.5. Concluding remarks

Our results illustrate two ways that the dynamics of a chemical reaction can be affected by a confining material, even when strong catalytic effects (via bonding with the surface) are absent. The first way is the effect of geometrical constraints, which we see partially in the dissociation of HI, and more clearly in the isomerization of 1,3-butadiene. In both examples we find that geometrical constraints are capable both of enhancing and hindering a chemical reaction. In the case of HI, the formation of the transition state structure is favored by the reduction of the pore size, and in the case of 1,3-butadiene, the automerization of the *s-gauche* conformer is also helped by it. The isomerization from *s-trans* to *s-gauche*-1,3-butadiene, however, is hindered.

A second way in which a material can affect the reaction dynamics (in absence of bonding with the surface) is by interacting with the reacting mixture in a way that favors the formation of an activated complex. This is illustrated both in the dissociation of HI, where the fluid–wall interaction of the transition state is more favorable than that of hydrogen iodide, and in the decomposition of formaldehyde, where the graphene sheet helps the transference of charge along the C–O bond. In this case, the effect on the reaction is similar to that of a solvent, as pointed out by Halls and Schlegel [44].

Both of the effects discussed above can actually be summarized into one if we invoke the ideas of TST. In

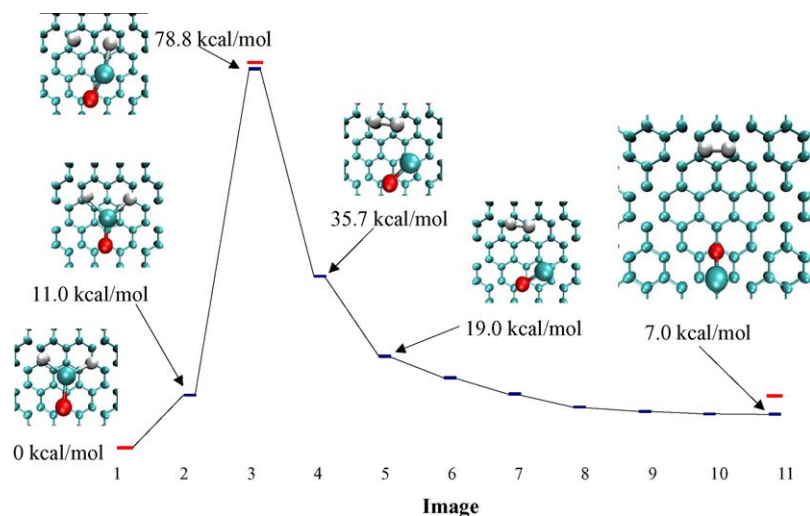


Fig. 10. Energy profile for the unimolecular decomposition of formaldehyde close to a graphene wall. Image 3 is the transition state. The bulk values for the transition state and the products are marked in red.

both cases, the confining environment favors or hinders the formation of the transition state either through steric hindrance (as in the isomerization of 1,3-butadiene), or through favorable fluid–wall interactions (as in the decomposition of formaldehyde), or both (as in the dissociation of HI). This interpretation is, of course, incomplete as TST is not applicable to all reactions, and we are not accounting for the possibility of strong catalytic effects. Therefore, there are still questions to answer, e.g. what is the relative importance of these factors for a reaction where the surface acts as a “true” catalyst? Also, the calculations shown for 1,3-butadiene and formaldehyde are done in the Henry’s law limit, and so they do not account for the influence of the local density on the reaction rate. These points will be considered in the next section.

4. Current research directions

As mentioned at the end of the previous section, there are still some questions we need to address if we want a complete picture of the effect of confinement on chemical reactions. Some of the problems we are currently working on include:

(1) The effect of confinement on conformational changes of various small molecules. Our results

for 1,3-butadiene are representative of situations where a molecule rearranges around a conjugated bond. We are currently studying the effect of confinement on molecular rearrangements for different bonding situations. In particular, we are studying the torsional potentials of *n*-butane, 1-butene, and 2-butene, in carbon slit-pores. Our preliminary results for *n*-butane indicate a similar effect of confinement: the barrier for the *anti-gauche* transition increases rapidly for pore sizes below 10 Å, whereas, the barrier for the *gauche-gauche* automerization decreases, and the *gauche* conformer shifts to lower torsion angles. The study of this effect for different molecules will shed light on cases where steric hindrance from the adsorbing material is important, and how it could be used to enhance the reactions desired, as well as hinder undesired ones.

(2) The effect of defects on the surface of the adsorbing material. We are currently studying the dissociation of formaldehyde, as well as other small molecules, over graphene surfaces with different kinds of defects such as vacancies and guest atoms or side chains. This kind of problem is both interesting and challenging because the reaction mechanism can be completely changed with respect to the bulk case, and it is possible for many different reaction pathways to appear. As an example, a dissociation pathway for formalde-

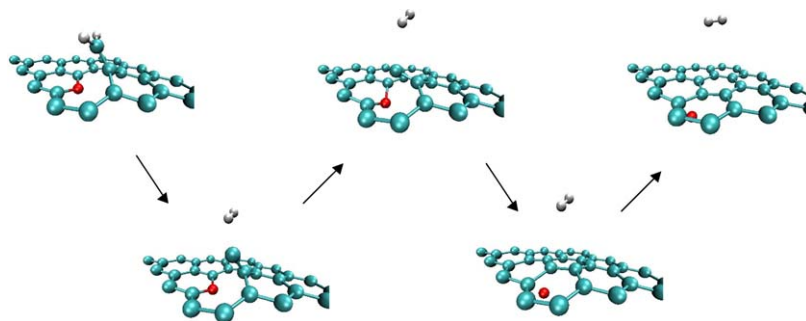


Fig. 11. An alternative pathway for the dissociation of formaldehyde over a graphene sheet with a single vacancy.

hyde over a vacancy in a graphene sheet is shown in Fig. 11. In this pathway, the oxygen atom goes through the hole in the graphene sheet, and the carbon atom ends up occupying the vacancy site, thus mending the sheet and leaving molecular hydrogen and atomic oxygen as products on different sides of the sheet. In order to study all the possible dissociation pathways for such systems, we are currently using the Laio–Parrinello metadynamics method [46,47] in addition to NEB.

- (3) The influence of the thermodynamic state of the system (temperature and density) on the reaction energy profile and the reaction rates. Although in the case of the dissociation of HI we account for the state of the system in the simulations, the model does not allow for deviations from TST, or for the influence of the local density on the molecular degrees of freedom. We are currently carrying out calculations using the Blue Moon molecular dynamics method [2,48,49] with reactive potentials fitted using the reaction path Hamiltonian approach [50] to obtain reaction rates for various reactions at different thermodynamic conditions, in order to address this problem.

Acknowledgements

This work was supported by grants from the National Science Foundation (CTS-0211792), the Department of Energy (DE-FG02-98ER14847) and a NATO Collaborative Linkage Grant (No. PST.CLG.978802). Supercomputer resources were provided under a NSF/NRAC Grant (No. NPA205), and by the High Performance Computing Centers at

North Carolina State University and University of North Carolina. The molecular graphics in this work were created using Visual Molecular Dynamics (VMD) [51].

References

- [1] J.K. Johnson, A.Z. Panagiotopoulos, K.E. Gubbins, *Mol. Phys.* 81 (1994) 717.
- [2] E.E. Santiso, K.E. Gubbins, *Mol. Simul.* 30 (2004) 699.
- [3] C.H. Turner, J.K. Johnson, K.E. Gubbins, *J. Chem. Phys.* 114 (2001) 1851.
- [4] C.H. Turner, J. Pikunic, K.E. Gubbins, *Mol. Phys.* 99 (2001) 1991.
- [5] C.H. Turner, K.E. Gubbins, *J. Chem. Phys.* 119 (2002) 6057.
- [6] W.A. Steele, *Interaction of Gases with Solid Surfaces*, Pergamon, Oxford, 1974.
- [7] J. Pikunic, R.J.M. Pellenq, K.T. Thomson, J.-N. Rouzaud, P. Levitz, K.E. Gubbins, *Stud. Surf. Sci. Catal.* 132 (2001) 647.
- [8] A.V. Shevade, S. Jiang, K.E. Gubbins, *J. Chem. Phys.* 113 (2000) 6933.
- [9] C.H. Turner, J.K. Brennan, J. Pikunic, K.E. Gubbins, *Appl. Surf. Sci.* 196 (2002) 366.
- [10] A.L. Smith, H.L. Johnson, *J. Am. Chem. Soc.* 74 (1952) 4696.
- [11] E.A. Guggenheim, *Mol. Phys.* 10 (1966) 401.
- [12] H.J.R. Guedes, Ph.D. thesis, Universidade Nova de Lisboa, Portugal, 1988.
- [13] K. Kaneko, N. Fukuzaki, K. Kakei, T. Suzuki, S. Ozeki, *Langmuir* 5 (1989) 960.
- [14] O. Byl, P. Kondratyuk, J.T. Yates, *J. Phys. Chem. B* 107 (2003) 4277.
- [15] M. Appl, *Ammonia*, Wiley, New York, 1999.
- [16] Y. Izumi, K. Urabe, *Chem. Lett.* 5 (1981) 663.
- [17] C.H. Turner, J.K. Brennan, J.K. Johnson, K.E. Gubbins, *J. Chem. Phys.* 116 (2002) 2138.
- [18] H. Eyring, *J. Chem. Phys.* 3 (1935) 107.
- [19] B.C. Garrett, D.G. Truhlar, *Transition state theory*, in: P.V.R. Schleyer, N.L. Allinger, T. Clark, J. Gasteiger, P.A. Kollman, H.F. Schaefer, III (Eds.), *Encyclopedia of Computational Chemistry*, Wiley, Chichester, 1998.

- [20] R.G. Parr, W. Yang, *Density-Functional Theory of Atoms and Molecules*, Oxford University Press, Oxford, 1989.
- [21] A.D. Becke, *Phys. Rev. A* 38 (1988) 3098.
- [22] C. Lee, W. Yang, R.G. Parr, *Phys. Rev. B* 37 (1988) 785.
- [23] D. Vanderbilt, *Phys. Rev. B* 41 (1990) 7892.
- [24] CPMD, Copyright IBM Corp. 1990–2003, Copyright MPI für Festkörperforschung Stuttgart 1997–2001, <http://www.cpmd.org>
- [25] S. Baroni, A. Dal Corso, S. de Gironcoli, P. Giannozzi, PWSCF, <http://www.pwscf.org>
- [26] A. Banerjee, N. Adams, J. Simons, R. Shepard, *J. Phys. Chem.* 89 (1985) 52.
- [27] S.R. Billeter, A. Curioni, W. Andreoni, *Comp. Mater. Sci.* 27 (2003) 437.
- [28] G. Mills, H. Jónsson, G.K. Schenter, *Surf. Sci.* 324 (1995) 305.
- [29] H. Jónsson, G. Mills, K.W. Jacobsen, Nudged elastic band method for finding minimum energy paths of transitions, in: B.J. Berne, G. Ciccotti, D.F. Coker (Eds.), *Classical and Quantum Dynamics in Condensed Phase Simulations*, World Scientific, Singapore, 1998.
- [30] G. Henkelman, B.P. Uberuaga, H. Jónsson, *J. Chem. Phys.* 113 (2000) 9901.
- [31] E.E. Santiso, A.M. George, M. Sliwinski-Bartkowiak, M. Buongiorno-Nardelli, K.E. Gubbins, *Adsorption* 11 (2005) 349.
- [32] G.B. Kistiakowsky, *J. Am. Chem. Soc.* 50 (1928) 2315.
- [33] B.R. Arnold, V. Balaji, J. Michl, *J. Am. Chem. Soc.* 112 (1990) 1808.
- [34] J.J. Fisher, J. Michl, *J. Am. Chem. Soc.* 109 (1987) 1056.
- [35] M.E. Squillacote, R.S. Sheridan, O.L. Chapman, F.A.L. Anet, *J. Am. Chem. Soc.* 101 (1979) 3657.
- [36] R. Engeln, D. Consalvo, J. Reuss, *Chem. Phys.* 160 (1992) 427.
- [37] L.A. Carreira, *J. Chem. Phys.* 62 (1975) 3851.
- [38] R.L. Lipnick, E.W. Garbisch Jr., *J. Am. Chem. Soc.* 95 (1973) 6370.
- [39] M.A. Murcko, H. Castejón, K.B. Wiberg, *J. Phys. Chem.* 100 (1996) 16162.
- [40] G.R. De Maré, Y.N. Panchenko, J.V. Auwera, *J. Phys. Chem. A* 101 (1997) 3998.
- [41] J.C. Sancho-García, A.J. Pérez-Jiménez, J.M. Pérez-Jordá, F. Moscardó, *Mol. Phys.* 99 (2001) 47.
- [42] J.C. Sancho-García, A.J. Pérez-Jiménez, F. Moscardó, *J. Phys. Chem. A* 105 (2001) 11541.
- [43] C.H. Choi, M. Kertesz, A. Karpfen, *Chem. Phys. Lett.* 276 (1997) 266.
- [44] M.D. Halls, H.B. Schlegel, *J. Phys. Chem. B* 106 (2002) 1921.
- [45] D.R. Guyer, W.F. Polik, C.B. Moore, *J. Chem. Phys.* 92 (1990) 3453.
- [46] A. Laio, M. Parrinello, *Proc. Natl. Acad. Sci. U.S.A.* 99 (2002) 12562.
- [47] M. Iannuzzi, A. Laio, M. Parrinello, *Phys. Rev. Lett.* 90 (2003) #238302.
- [48] G. Ciccotti, M. Ferrario, *J. Mol. Liq.* 89 (2000) 1.
- [49] G. Ciccotti, M. Ferrario, *Mol. Simul.* 30 (2004) 787.
- [50] W.H. Miller, N.C. Handy, J.E. Adams, *J. Chem. Phys.* 72 (1980) 99.
- [51] W. Humprey, A. Dalke, K. Schulten, *J. Mol. Graphics* 14 (1996) 33–38.